Bioactive Materials 6 (2021) 1689–1698

Contents lists available at ScienceDirect

Bioactive Materials

journal homepage: www.sciencedirect.com/journal/bioactive-materials

Modified hyaluronic acid hydrogels with chemical groups that facilitate adhesion to host tissues enhance cartilage regeneration

Jiaqing Chen [a], Jiabei Yang [a], Li Wang [a], Xuewei Zhang [a], Boon Chin Heng [b], Dong-An Wang [c], Zigang Ge [a,*]

[a] Department of Biomedical Engineering, College of Engineering, Peking University, Beijing, 100871, PR China
[b] School of Stomatology, Peking University, Beijing, 100081, PR China
[c] Department of Biomedical Engineering, College of Engineering, City University of Hong Kong, Hong Kong SAR, PR China

ARTICLE INFO

Keywords:
Cartilage regeneration
Hydrogel
Adhesion
Schiff base reaction
Hyaluronic acid
Aldehyde

ABSTRACT

Stable integration of hydrogel implants with host tissues is of critical importance to cartilage tissue engineering. Designing and fabricating hydrogels with high adhesive strength, stability and regeneration potential are major challenges to be overcome. This study fabricated injectable adhesive hyaluronic acid (HA) hydrogel modified by aldehyde groups and methacrylate (AHAMA) on the polysaccharide backbone with multiple anchoring mechanisms (amide bond through the dynamic Schiff base reaction, hydrogen bond and physical interpenetration). AHAMA hydrogel exhibited significantly improved durability and stability within a humid environment (at least 7 days), together with higher adhesive strength (43 KPa to skin and 52 KPa to glass), as compared to commercial fibrin glue (nearly 10 KPa) and HAMA hydrogel (nearly 20 KPa). The results showed that AHAMA hydrogel was biocompatible and could be easily and rapidly prepared *in situ*. *In vitro* cell culture experiments showed that AHAMA hydrogel could enhance proliferation (1.2-folds after 3 days) and migration (1.5-folds after 12 h) of bone marrow stem cells (BMSCs), as compared to cells cultured in a culture dish. Furthermore, in a rat osteochondral defect model, implanted AHAMA hydrogel significantly promoted integration between neo-cartilage and host tissues, and significantly improved cartilage regeneration (modified O'Driscoll histological scores of 16.0 ± 4.1 and 18.3 ± 4.6 after 4 and 12-weeks of post-implantation in AHAMA groups respectively, 12.0 ± 2.7 and 12.2 ± 2.8 respectively in HAMA groups, 9.8 ± 2.4 and 11.5 ± 2.1 respectively in untreated groups). Hence, AHAMA hydrogel is a promising adhesive biomaterial for clinical cartilage regeneration and other biomedical applications.

1. Introduction

Integration between implanted hydrogel scaffolds with host tissues is essential for efficient tissue regeneration, particularly for cartilage, which could facilitate the healing process and recovery of mechanical function [1–3]. Poor integration between implanted biomaterials and native cartilage often causes tissue fibrosis, leading to inefficiency in transferring mechanical loads and failure of integration of neo-cartilage with native cartilage, ultimately resulting in failure of cartilage regeneration [4,5]. Nevertheless, good and stable integration between implanted biomaterials and native cartilage remains a formidable challenge.

For cartilage regeneration, existing adhesive hydrogels are far from ideal, and should be more biocompatible, easy to use, cost-effective and efficient in enhancing regeneration [6]. Commercial-available adhesives, such as fibrin glue TISSEEL (Baxter) [7] and polyethylene glycol–based adhesive hydrogels, such as COSEAL (Baxter) and DUEASEAL (Confluent) [8], have demonstrated weak adhesion to tissues, and tend to decrease significantly under wet conditions, which make these unsuitable for cartilage tissue engineering [9]. Cyanoacrylate adhesives, induce cytotoxic reaction, are incompatible with wet surfaces [10], and are generally unsuitable for cartilage tissue engineering. Adhesive hydrogels utilized in research can usually be divided into two types according to adhesion mechanisms, (a) formation of an interpenetrating network of mechanical interlocks between tissues and materials, (b) formation of chemical bonds between tissues and materials through various functional groups, such as aldehyde, sulfonate, catechol, and imine groups, or even with some tissue affinity peptides [1,11,12].

* Corresponding author.
E-mail address: gez@pku.edu.cn (Z. Ge).

https://doi.org/10.1016/j.bioactmat.2020.11.020
Received 17 May 2020; Received in revised form 11 November 2020; Accepted 12 November 2020

Hydrogels with mechanical interlocking properties are usually photo-crosslinked biomaterials [13–15], alginate gels or fibrin gels [16,17]. However, without stable adhesion to cartilage, few research studies have used this strategy to promote cartilage regeneration *in vivo*. Other type of hydrogels with chemical binding properties are mostly modified with dopa (or catechol) or are able to form amide bond with tissues in cartilage regeneration [5,18,19]. Materials modified with dopa are easily oxidized at elevated pH values (pH from 3 to 8) [20], leading to decreased adhesive strength and biocompatibility [20,21]. Schiff base reactions are widely used to form amide bonds, which are biocompatible with good adhesive strength [4,5,22]. However, hydrogel scaffolds that adhere to cartilage by amide bonds, often need two/multiple components to gel, which complicate surgical operations, as well as have too fast degradation rate, leading to unstable adhesion over a long-time scale [23]. Besides adhesive strength, the efficacy in promoting cartilage regeneration should also be considered.

Hyaluronic acid (HA), which forms the molecular backbone of proteoglycan complexes [24], is composed of repeating units of *N*-acetyl-D-glucosamine and D-glucuronic acid [25]. It contains carbon-carbon bonds of cisdiol groups, which could be easily oxidized to generate reactive aldehyde groups to form amide bonds via the Schiff base reaction [25,26]. Due to good biocompatibility and bioactive properties, HA is widely utilized for cartilage regeneration. It is known to promote proliferation of chondrocytes and MSCs [27,28], modulate inflammation [12,29], and promote cartilage regeneration [30]. Strategies applied in chemically binding HA to cartilage often utilize HA affinity peptides [12,31] and HA modified with aldehyde groups [18,19]. HA modified with affinity peptides can enable HA to localize and stay on the cartilage surface. However, animal studies did not show significant improvements [12]. The shortcoming of HA modified with aldehyde groups, i.e. HA (AHA), is that it cannot self-gel and needs to mix with other components to gel, such as HA modified with adipic dihydrazide or PRP [5,18,19]. This not only consumes the aldehyde groups, decreasing adhesive capacity to host tissues, but also results in the release of potentially toxic degradation products and complicates the surgical operation procedure [32].

In this study, we developed a modified HA methacrylate hydrogel with aldehyde groups to facilitate adhesion to host tissues, and promote cartilage regeneration (AHAMA). Firstly, HA was chemically cleaved by sodium periodate to introduce aldehyde groups that facilitate adhesion to host tissues. Then methacrylated AHA was synthesized for crosslinking and physical interpenetration after oxidation of carbon-carbon bonds of cisdiol groups by sodium periodate, avoiding the potential oxidation of double bonds. By incorporating methacrylate, AHAMA could self-gel, thereby overcoming the problems of stability, degradation, and complications with multiple component materials. Through incorporation of both aldehyde groups and methacrylate, AHAMA hydrogels could be localized on the cartilage surface with multiple anchoring mechanisms (amide bond through the dynamic Schiff base reaction, hydrogen bond and physical interpenetration) (Fig. 1a). Upon introducing the AHAMA hydrogel to the cartilage surface, we observed that it could stably adhere to native cartilage tissue and promote cartilage regeneration. In this study, the microstructural properties, mechanical and adhesive properties, biocompatibility and biological effects on MSCs, as well as the efficacy of adhesive AHAMA hydrogels in promoting orthotopic cartilage regeneration in a rat cartilage defect model *in vivo* were systematically evaluated.

2. Material and methods

2.1. Materials

Sodium hyaluronate (Mw 100,000–200,000, H-0443571, HEOWNS, Tianjin, China), Sodium periodate (110,023-5 g, TONG GUANG FINE CHEMICAL COMPANY, Beijing, China), Ethylene glycol (10009818, HUSHI, Shanghai, China), Methacrylic anhydride (M – 58350, HEOWNS, Tianjin, China) and other regents were commercially-available and used as received.

2.2. Fabrication and characterization of HAMA and AHAMA hydrogel

AHA was synthesized as previously described [26,33]. Briefly, 1 g of HA was dissolved in 100 ml of water and agitated until the HA was completely dissolved. Then 5 ml of 0.5 M sodium periodate was added dropwise and agitated with a speed of 250 rpm for 2 h at room temperature in the dark. 1 ml of ethylene glycol was then added to inactivate the unreacted periodate for 1 h. After exhaustive dialysis against H_2O for 3 days, AHA was obtained by freeze-drying.

Methacrylated HA and AHA were synthesized as previously reported [34]. The HA and AHA were modified with double bonds by reacting with methacrylate. Briefly, 1 g of HA or AHA was dissolved into 100 ml of water and agitated until completely dissolved. Then, 1 ml of methacrylate was added and the reaction was maintained for 12 h with pH at 8–8.5. The whole process was carried out on ice, including the dissolution and reaction. After the reaction, the solution was dialyzed for 2 d and freeze-dried. The percentage of double bond was quantified by ^{1}HNMR dissolved in D_2O. The aldehyde content of AHAMA was quantified using *tert*-butyl carbazate and trinitrobenzene sulfonic acid (TNBS) solution [25].

HAMA or AHAMA were dissolved in PBS solution (3% w/v) with

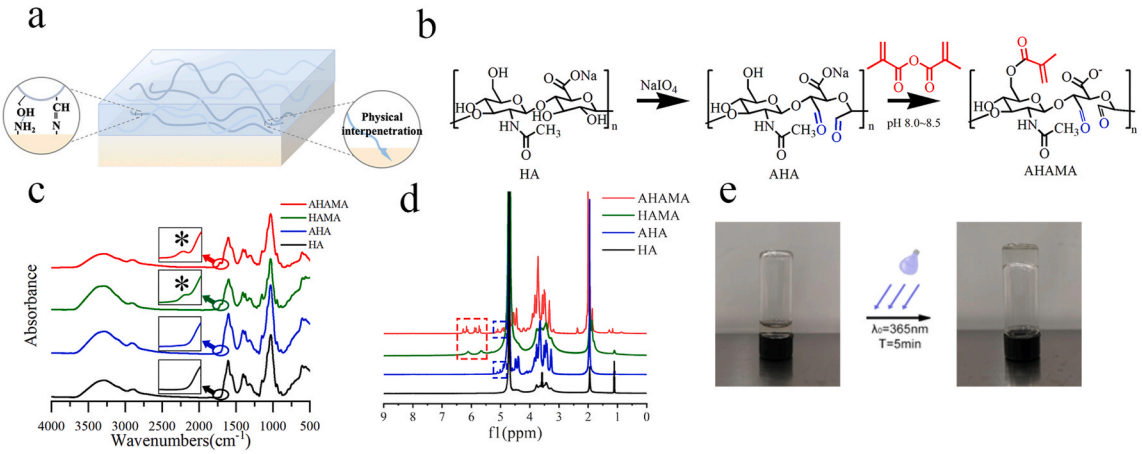

Fig. 1. Fabrication of AHAMA hydrogel. (a) Schematic illustration of adhesive hydrogel bonding to tissue. (b) Schematic illustration of the synthetic AHAMA. (c) FTIR spectra of the HA, AHA, HAMA and AHAMA hydrogels. * represents new peak appearing due to the stretching band of the C=C bond. (d) ^{1}H NMR spectra of HA, AHA, HAMA and AHAMA hydrogels in D_2O (500 MHz). (e) Gelation of the AHAMA hydrogel.

0.1% (w/v) of the photoinitiator 2-Hydroxy-4′-(2-hydroxyethoxy)-2-methylpropiophenone (I2959, Aladdin, H137984). Then the hydrogel was formed by exposure to 365 nm ultraviolet (UV) light (10 mW/cm^2) for 5min.

The microstructures and pore sizes of HAMA and AHAMA hydrogels were characterized by SEM. The samples were mounted and sputter coated with gold–palladium, before being imaged with scanning electron microscopy (SEM; HITACHI S4800) at an accelerating voltage of 5 kV. The pore size was analyzed using the Nano Measurer software. Young's modulus was measured by a Nanoindenter (Piuma Chiaro, OPTICS II, Netherlands) with a falling speed of 10 μm/s. Characterization of HAMA and AHAMA was performed with a Fourier-transform infrared spectrometer (FTIR, Nicolet is50, Thermo Fisher, USA) and ^{1}H NMR (Bruker-500, AVANCE III, Switzerland). The porosity was calculated as follows:

$$Porosity = \frac{W_s - W_d}{\rho V},$$

where ρ is the density of ethanol at 37 °C and V is the volume of the materials, W_s and W_d represent the mass of the swollen and dried materials, respectively. The Swelling ratio was calculated as follows:

$$Swelling\ ratio = \frac{W_s - W_d}{W_d}.$$

Adhesive strength was measured using the lap-shear test by uniformly adding 100 μL of pregel solution to amino-treated glass slices (tbdscience, FISH0010). The test samples were exposed to 365 nm ultraviolet (UV) light (10 mW/cm^2) for 5min to allow the pregel solution to gel *in situ* (bonded area of 25 mm × 25 mm). Then the samples were pulled to failure by a universal testing machine (Instron5969, USA) equipped with a load cell of maximum 100 N capacity with a crosshead speed of 1 mm/min. The adhesive strength was calculated by the maximum stress divided by the bonded area. The force (F) versus extension (δ) curves were integrated to determine the work of adhesion (W_{adh}) by the equation [35]:

$$W_{adh} = \frac{\int F d\delta}{A_{max}}$$

Samples were placed into a humidity chamber before being measured. Porcine skin was chosen to mimic the adhesion to human tissues (bonded area of 5 mm × 5 mm).

2.3. Cell isolation and culture

After obtaining approval from the Peking University Animal Center (COE-GeZ-3 and COE-GeZ-6), MSCs were isolated from the bone marrow of pigs (Yorkshire, 10–12 months). MSCs were cultured in growth medium composed of Dulbecco's modified Eagle's medium (DMEM, Gibco-Invitrogen, China) supplemented with 10% (v/v) fetal bovine serum (FBS) (Gibco-Invitrogen), 100 μg/ml of streptomycin, and 100 μg/ml of penicillin at 37 °C within a humidified 5% CO_2 atmosphere. Non-adherent cells were washed away after 72 h. When adherent cells reached 80% confluence, they were detached using 0.05% (w/v) of trypsin (Gibco-Invitrogen) for further passage. Passage 1 MSCs were frozen down in 90% (v/v) fetal bovine serum (life) and 10% (v/v) dimethysulphoxide. When MSCs proliferated to Passage 5, cells were seeded in HAMA or AHAMA hydrogels.

2.4. Cytocompatibility and migration of AHAMA hydrogel

The cytocompatibility of AHAMA hydrogel was evaluated by live/dead staining assay and cell counting kit-8 (Solarbio, CA1210). For live/dead staining, 2 × 10^5 cells were mixed in 50 μL of HAMA or AHAMA pregel solution before gelation. After being cultured in medium for 24 h, HAMA and AHAMA hydrogels were stained with 2 μg/ml of Fluorescein Diacetate (FDA, F7378, Sigma) at 37 °C for 15min and 5 μg/ml of Propidium Iodide (PI, P4170, sigma) at 37 °C for 5min, before being evaluated under laser scanning confocal microscopy (Andor) at an excitation wavelength of 488 nm, and emission wavelengths from 550 to 670 nm. For cytotoxicity assay, 1 × 10^3 MSCs were seeded in 96-well plates with 100 μL of medium in each well and incubated at 37 °C for 24 h. Then the medium was changed with hydrogel extracts every day until analysis (1 day or 3 days). Hydrogel extracts were prepared according to the GB/T 16886.5 protocol. Briefly, 100 μL of hydrogel was incubated with 1 ml DMEM culture medium (containing 10% v/v FBS) at 37 °C for 24 h. Six replicates samples were collected for each group, at each timepoint. For the cell migration assay, BMSCs were seeded in 6-well plates and cultured until confluent. The confluent cell monolayer was then scratched with a 200 μL pipette tip across to the center to create a cross. Then 100 μL of hydrogel was placed into the scratched well. After being cultured for 6 and 12 h, the cells were imaged and quantitatively analyzed.

2.5. F-actin fluorescence staining

F-actin fluorescence staining was used to evaluate BMSCs morphology on the hydrogel surface. After 1 d culture, samples were rinsed, fixed with 4% (w/v) paraformaldehyde and permeabilized with 1.5% (w/v) Triton-X100. F-actin was stained with rhodamine-conjugated phalloidin (Sigma). Cell nuclei were stained with 4, 6-diamidino-2-phenylindole (DAPI; Vector Laboratories). Microscopic imaging was performed on a Revolution XD spinning disk confocal microscope (Andor) at an excitation wavelength of 405 nm (DAPI) and emission wavelength 561 nm (rhodamine-conjugated phalloidin).

2.6. Chondrogenic differentiation of MSCs

50 μL of pre-gel mixed with 2.5 × 10^5 MSCs were exposed to UV light for 5 min. Hydrogels containing cells were placed in chondrogenic differentiation medium composed of high glucose DMEM (HyClone, China), 10^{-7} M of dexamethasone, 50 μg/ml of ascorbic acid, 1 mM of sodium pyruvate (Sigma-Aldrich, China), 4 mM of proline (Sigma-Aldrich, China) and 1% (v/v) of ITS + premix. Samples were cultured in chondrogenic differentiation medium for 7 and 14 days with medium change every three days. The primer sequences used for RT-PCR to detect functional gene are listed in Table s1.

2.7. Cartilage regeneration in the rat defect model

All experiments were conducted according to protocols established by the Institutional Animal Care and Use Committee of Peking University (COE-GE-3 and COE-GE-6). The rats were randomly assigned into three groups (10 weeks of age): Untreated groups (defects left empty without implantation, n = 6 joints at each time point), HAMA groups (defects implanted with HAMA hydrogel, n = 6 joints at each time point), AHAMA groups (defects implanted with AHAMA hydrogel, n = 6 joint at each time point). After anesthesia, a midline incision was made in front of the knee joint. Defects of 1.5 mm in diameter and 1.5 mm in depth were created at the middle of the femoral trochlear of the knee joint. 50 μL HAMA or AHAMA solution was injected into the defect, and then exposed to 365 nm of ultraviolet (UV) light (10 mW/cm^2, 5 min) to fix the hydrogel within the cartilage defect. The rats were sacrificed at 4 weeks and 12 weeks after surgery, and the implants were harvested together with the surrounding tissues and the 6 explanted knee joints of each group were evaluated histologically. The harvested tissue specimens were fixed in 4% (w/v) paraformaldehyde at 4 °C for 24 h and decalcified for 1 month at 4 °C, before being embedded in paraffin and processed using standard histological procedures.

2.8. Histology and immunohistochemistry staining

The histological sections (5 μm thick) were subjected to H&E and Safranin O staining, as well as immunohistochemical staining for detection of collagen type I and II. For H&E staining, tissue sections were stained in Harris hematoxylin solution for 10 min, and then counterstained in eosin-phloxine solution. For safranin O staining, tissue sections were stained in fast green (0.05%, w/v) for 5 min, and then counterstained in safranin O (0.1%, w/v) solution for 5 min. For the immunohistochemical staining of rat samples, tissue sections were incubated with hydrogen peroxide to block endogenous peroxidase, followed by heat treatment at 60 °C for 1 h to retrieve antigen. Monoclonal antibodies against collagen type I (ab34710, Abcam), and collagen type II (ab34712, Abcam) were then added and incubated at 4 °C overnight, followed by addition of a biotinylated goat anti-mouse IgG antibody. After incubation with streptavidin peroxidase, the sections were stained with 3, 3′-diaminobenzidine as the chromogenic agent. Mayer's hematoxylin (AppliChem, A0884) was applied for cell nuclei counterstaining. The tissues were then assessed by ICRS Macroscopic scoring and Modified O'Driscoll histological scoring (Table s2 and s3, each sample judged by two individuals).

2.9. Statistical analysis

The data were expressed as mean ± standard deviation (SD). Statistical analyses were performed using IBM SPSS 20 software (one-way ANOVA, (*) for $p < 0.05$, (**) for $p < 0.01$, and (***) for $p < 0.001$).

3. Results

3.1. Fabrication and characterization of AHAMA hydrogel

Following the fabrication process illustrated in Fig. 1b, AHAMA was successfully obtained, as confirmed by FTIR and ^{1}H NMR. The stretching band of the C═C bond from methacrylate at 1700 cm^{-1} was detected in AHAMA and HAMA (Fig. 1c). Two new peaks at 5.7 ppm and 6.1 ppm were observed on the ^{1}H NMR spectra of AHAMA and HAMA, which correspond to protons within the C═C bond of methacrylate (Fig. 1d). The methacrylate modification levels of HAMA and AHAMA were estimated to be 26% and 24% respectively, based on the ^{1}H NMR spectrum (Fig. 1d). Two other new peaks at 4.9 ppm and 5.0 ppm were observed on the ^{1}H NMR spectra of AHAMA and AHA, which corresponded to the hemiacetalic protons formed from the aldehyde groups and neighboring hydroxyl groups (Fig. 1d) [36]. The oxidation level of AHAMA was 36%, as quantified by measuring the number of aldehydes using t-butylcarbazate and 2,4,6 trinitrobenzene-sulfonic acid (TNBS). Both HAMA and AHAMA were gelled by exposure to UV light (365 nm, 10 mW/cm^2) for 5 min (Fig. 1e).

The microstructure of the HAMA and AHAMA hydrogels were porous with good connectivity, as shown by SEM images and porosity tests (Fig. 2a and b). The average pore size of the AHAMA hydrogel was significantly higher than HAMA (352 ± 27 μm for AHAMA and 245 ± 38 μm for HAMA, Fig. 2c). As compared to the HAMA hydrogel, AHAMA hydrogel had relatively lower Young's modulus (nearly 10 KPa, Fig. 2d), due to the ring opening by sodium periodate. Both HAMA and AHAMA hydrogels displayed uniform Young's modulus (Fig. s1). The swelling ratio of AHAMA quickly increased to 27 after 10 min immersion in PBS, and then continued to rise to 58 after 24 h (Fig. 2e and Fig. s2). The swelling ratio of HAMA increased to 19 after 10 min and this level was maintained over time (Fig. 2e and Fig. s2).

3.2. Adhesive strength and tissue integration of AHAMA hydrogel

AHAMA hydrogel exhibited good adhesive strength to glass and porcine skin. The AHAMA hydrogel firmly adhered to the merged glass, with loading of 2 kg after gelation and 3 kg after 1 day (Fig. s3a). To quantitatively detect the adhesive strength of AHAMA to glass, the lap-shear test was performed (Fig. s3b), with fibrin glue and HAMA hydrogel setting as contrast. Compared to fibrin glue and HAMA hydrogel, AHAMA hydrogel showed significantly higher adhesive strength and work of adhesion at every time point (Fig. s3b and s3c). After 7 days, AHAMA still showed high adhesive strength to glass (nearly 19 KPa, Fig. s3e). In addition, after breakage of the two glass slices, the hydrogels of all samples were uniformly distributed on two slices, which

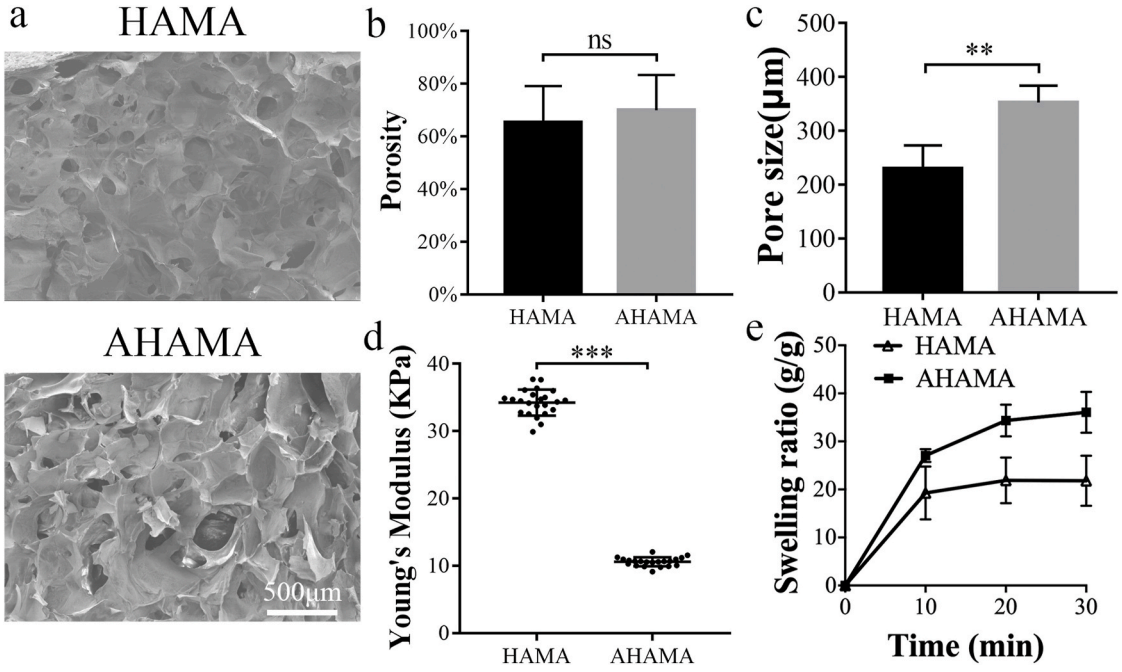

Fig. 2. Characterization of the AHAMA hydrogel. (a) SEM images of the inner structure of HAMA and AHAMA hydrogels. Scale bars: 500 μm. (b) Porosity of HAMA and AHAMA hydrogels (n = 4). (c) Pore sizes of HAMA and AHAMA hydrogels (n = 4). (d) Young's modulus of HAMA and AHAMA hydrogels measured by a nanoindenter (n = 20). (e) Swelling ratio of HAMA and AHAMA hydrogels from 10min to 30min (n = 6, mean values ± SD, *P < 0.05, **P < 0.01, ***P < 0.001).

indicated that the hydrogel broke before it separated from the glass (Fig. s4). Therefore, the actual binding strength of hydrogel-glass is higher than the test value. Porcine skins were used to measure adhesive strength of AHAMA hydrogel to tissue (Fig. 3a). Adhesive strength and work of adhesion of AHAMA hydrogel to porcine skin was higher than fibrin glue and HAMA hydrogel at every time point (Fig. 3b and c). Different from glass, AHAMA showed the highest adhesive strength to porcine skin on day 3 (Fig. 3b and c). SEM imaging was used to characterize hydrogel adhesion to porcine skin and cartilage. A noticeable difference was observed between HAMA hydrogel and porcine skin or cartilage due to the absence of covalent bonds (Fig. 3d and e), whereas AHAMA hydrogel tightly adhered to porcine skin and cartilage without any cracks (Fig. 3d and e).

3.3. Biocompatibility and influence on cell morphology of AHAMA hydrogel

The biocompatibility of AHAMA hydrogels was assessed using Live/Dead staining and CCK-8 assay, respectively. Live/Dead staining showed a high viability of BMSCs in AHAMA hydrogel, with relatively stronger staining than BMSCs cultured in alginate hydrogel at 24 h after seeding (Fig. 4a). The cell viability of BMSCs cultured for 24 h in media containing hydrogel extracts of alginate, HAMA and AHAMA were similar to MSCs cultured on culture dishes with normal proliferation media on day 1 (Fig. 4b). However, by day 3, HAMA and AHAMA groups displayed significantly higher cell viability than the control groups (Fig. 4b).

Cell morphology was characterized by directly taking SEM images and performing cell cytoskeleton staining to investigate the effects of hydrogel on MSCs. SEM results showed that MSCs seeded on AHAMA hydrogel exhibited normal stretching, similar to HAMA groups and culture dish groups (Fig. 4c). F-actin and nuclei staining showed a similar trend, MSCs seeded on the surface of HAMA and AHAMA hydrogels exhibited normal stretching, similar to culture dishes (Fig. 4d).

The cell migration test showed that media containing AHAMA hydrogel could significantly enhance cell migration after 12 h (Fig. 4e and Fig. s6).

3.4. Inducement of MSCs chondrogenesis in AHAMA hydrogel

After cocultured with MSCs about 7 days in chondrogenic differentiation medium, groups of AHAMA hydrogel could partially enhance the gene expression of SOX9 and decrease the gene expression levels of COL I, as compared to the positive control group, even though differences were insignificant (Fig. 5a). Additionally, groups of AHAMA did not significantly change the gene expression levels of COL II, ACAN and COL X, as well as deposition of glycosaminoglycan (Fig. 5a and b). After coculture with MSCs for 14 days in chondrogenic differentiation medium, groups of AHAMA hydrogel significantly enhanced the gene expression of COL II (25.4 ± 3.1-folds) and ACAN (22.5 ± 4.3-folds), but did not significantly change the gene expression of SOX9, COL I and COL X, as compared to the positive control group (Fig. 5a). Compared to the HAMA groups, the AHAMA groups showed slight enhancement, as seen with staining of Col II after 14 days of coculture, and similar staining results with H&E and Alcian blue (Fig. s7).

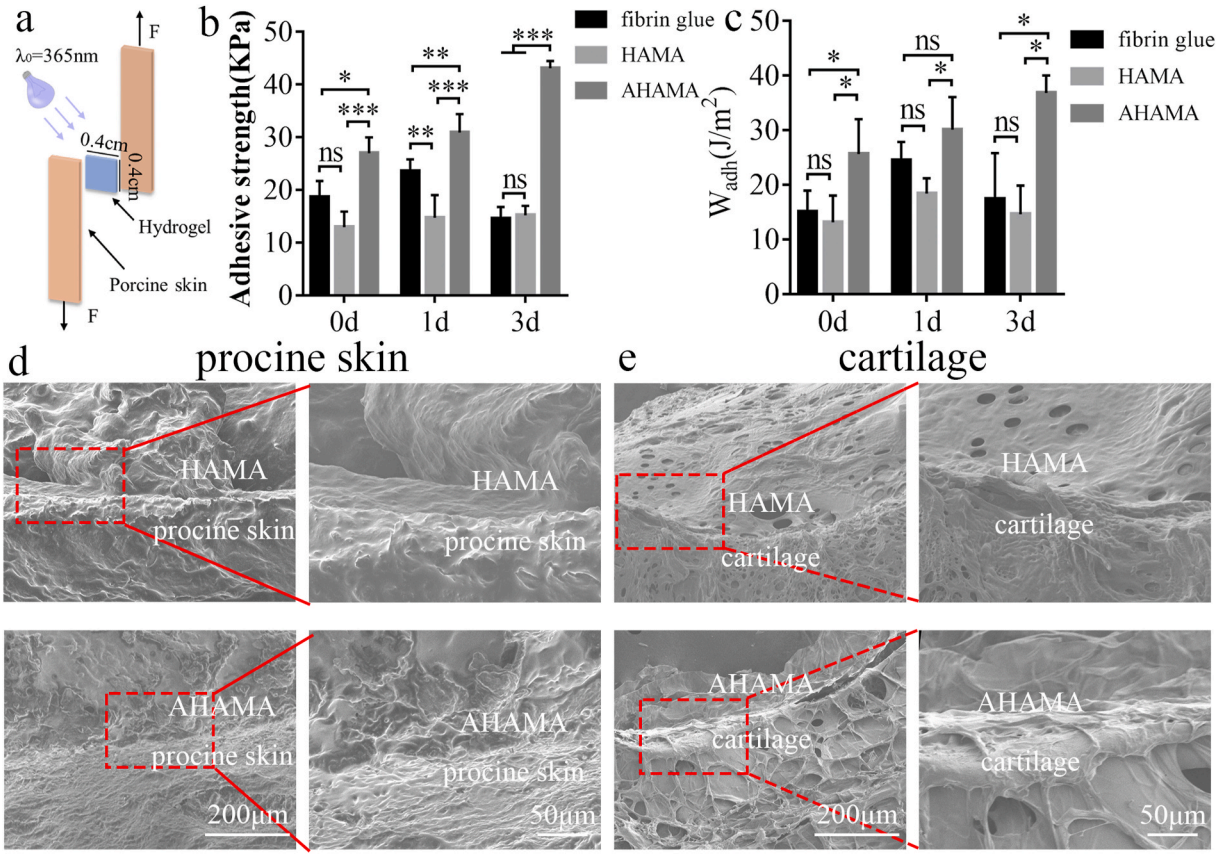

Fig. 3. Adhesive strength of the AHAMA hydrogel. (a) Schematic illustration of the lap-shear test on porcine skin. (b) Adhesive strength of fibrin glue, HAMA and AHAMA hydrogels to porcine skin (n = 3). (c) Work of adhesion of fibrin glue, HAMA and AHAMA hydrogels to porcine skin (n = 3). (d) SEM images of HAMA and AHAMA hydrogels adhered to porcine skin. Scale bars: left: 200 μm; right (enlarged area): 50 μm. (e) SEM images of HAMA and AHAMA hydrogels adhered to cartilage. Scale bars: left: 200 μm; right (enlarged area): 50 μm (Mean values ± SD, *P < 0.05, **P < 0.01, ***P < 0.001).

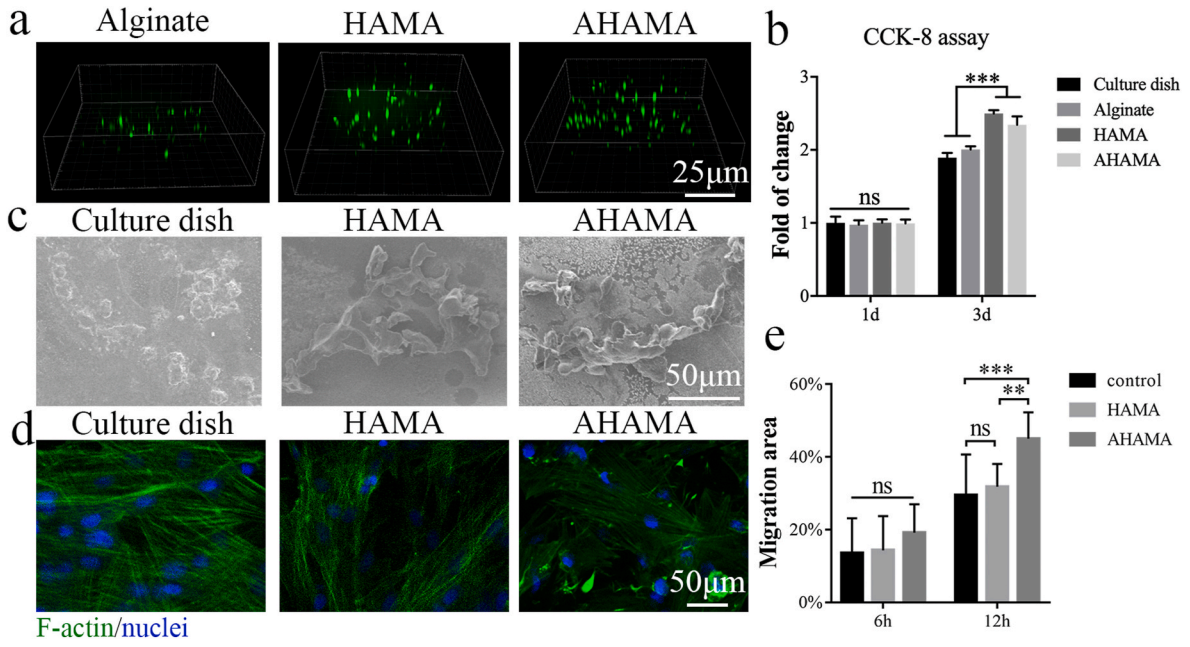

Fig. 4. Biocompatibility and cell morphology. (a) Live-dead staining confocal images of MSCs *in situ* encapsulated in alginate, HAMA and AHAMA hydrogels after culturing for 24 h. FDA for live cells (green) and PI for dead cells (red). Scale bar: 25 μm. (b) Evaluation of cell viability (CCK-8 assay) of MSCs on culture dish, alginate, HAMA and AHAMA hydrogels after 1 d and 3 d of culture (n = 6). (c) SEM image showing the morphology of MSCs seeded on the surface of culture dish, HAMA and AHAMA hydrogels. Scale bar: 50 μm. (d) F-actin and nuclei staining 1 day after seeding MSCs on the surface of culture dish, HAMA and AHAMA hydrogels. Rhodamine phalloidin for F-actin (green) and DAPI for cell nuclei (blue). Scale bar: 50 μm. (e) Mean migration area of MSCs (n = 6). (Mean values ± SD, *P < 0.05, **P < 0.01, ***P < 0.001).

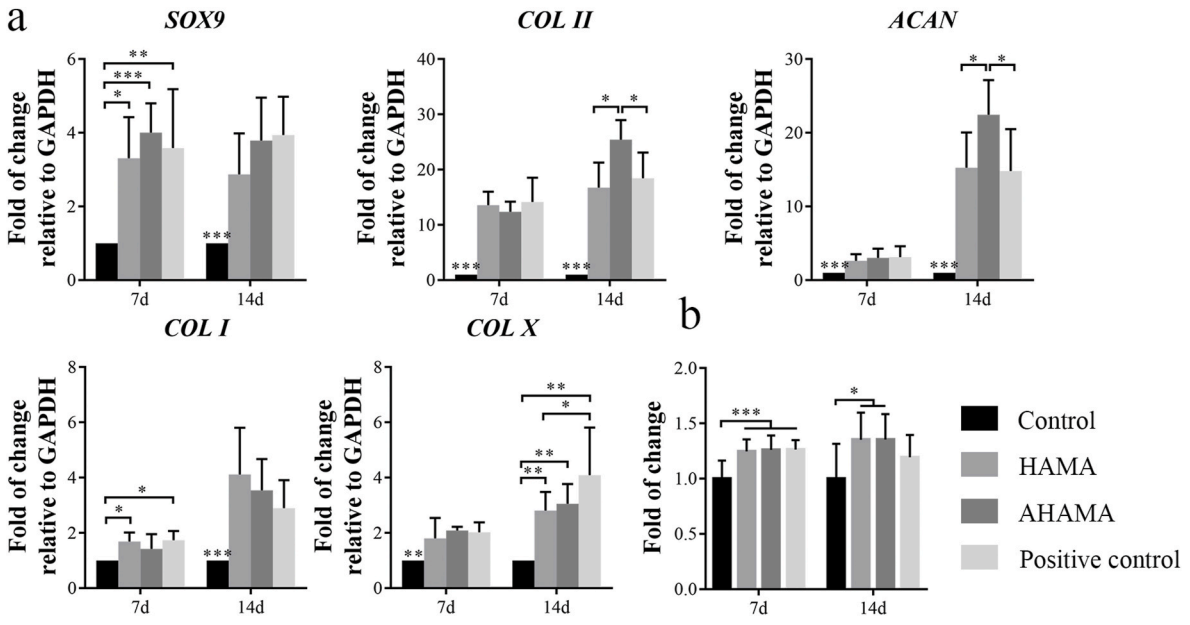

Fig. 5. Inducement of MSCs chondrogenesis in AHAMA hydrogel. (a) Gene expression levels of SOX9, COL II, ACAN, COL I and COL X of MSCs seeded in AHAMA hydrogel (n = 6). (b) Quantitative analyses of glycosaminoglycans contents of MSCs seeded in AHAMA hydrogel (n = 6, Mean values ± SD, *P < 0.05, **P < 0.01, ***P < 0.001).

3.5. *In vivo* cartilage defect regeneration

The capacity of AHAMA hydrogel in promoting host tissue cartilage regeneration was investigated in a rat osteochondral defect model, which was 1.5 mm in diameter and 1.5 mm in depth. The gross appearance revealed almost complete filling of the chondral defects in HAMA and AHAMA groups, as compared with the Untreated groups, in which tissue indentation at the defect site was obvious at 4 weeks post-implantation (Fig. 6a). After 12 weeks of cartilage regeneration, the AHAMA groups revealed a more glossy and well-integrated morphology, with no obvious boundaries at some sites. However, some small defects were observed in the HAMA and Untreated groups. The ICRS macroscopic score (total points were 12) was highest in the AHAMA groups after 4 and 12 weeks of regeneration (9.2 ± 1.2 and 10.5 ± 1.0), followed by the HAMA group (7.7 ± 0.7 and 7.5 ± 1.3) and Untreated group (4.3 ± 1.6 and 7.2 ± 1.0) (Fig. 6b).

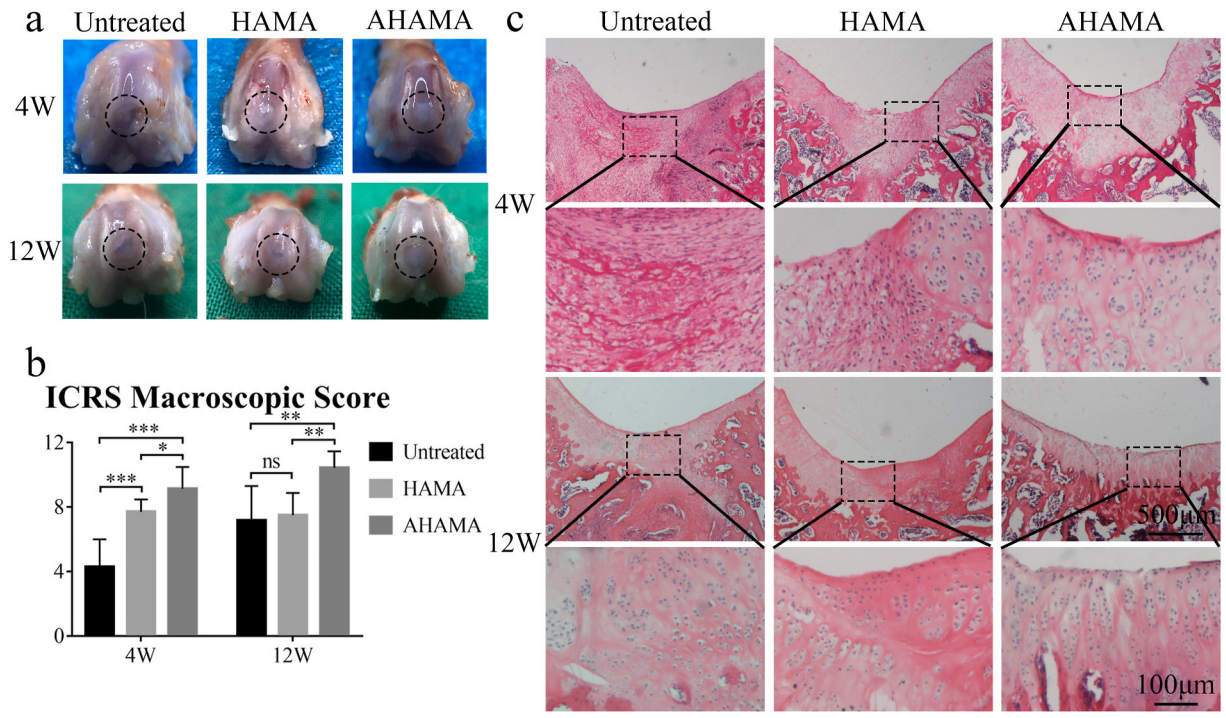

Fig. 6. Cartilage regeneration *in vivo*. (a) Macroscopic appearance of the cartilage defect at 4- and 12-weeks post-surgery. (b) ICRS macroscopic scores of Untreated, HAMA and AHAMA groups at 4- and 12-weeks post-surgery (n = 6, mean values ± SD, *P < 0.05, **P < 0.01, ***P < 0.001). (c) H&E staining of repaired cartilage after 4- and 12-weeks post-surgery. Scale bars: up: 500 μm; down (enlarged area): 100 μm.

H&E staining was performed to assess the cell distribution, hypocellularity, structural integrity and tissue regeneration. After 4 weeks post-implantation, much fibrous tissues were observed in the Untreated groups, with unevenly distributed clustered cells. Some fibrous tissues and cartilage-like tissues were also observed in the HAMA groups, with slight disruption. The implanted AHAMA scaffold exhibited better cartilage regeneration with smooth cartilage surface (Fig. 6c). After 12 weeks post-implantation, the boundary between the neo-tissue and native cartilage was still significant in the Untreated and HAMA groups, and some cells exhibited columnar arrangement, while others were still clustered. The AHAMA groups exhibited excellent tissue integration with native cartilage, and had more columnar arrangements of cells, close to healthy cartilage (Fig. 6c and Fig. s8). Safranin-O and immunohistological staining of collagen type II and I were performed to assess the cellular matrix, structural integrity and tissue regeneration. The stronger Safranin-O and collagen type II staining, and weaker collagen type I staining were found in both AHAMA groups after 4- and 12-weeks post-implantation, with new smooth and continuous tissue surfaces and tidelines, which demonstrated that the newly formed tissue was mainly hyaline cartilage, very similar to native cartilage (Fig. 7a and b and Fig. s9). The Untreated and HAMA groups did not show good cartilage regeneration (Fig. 7a and b and Fig. s9). Modified O'Driscoll 24-point histological scoring (Table s3) showed the same trend, with AHAMA gaining significantly higher score after 4-weeks post-implantation (16.0 ± 4.1) and 12-weeks post-implantation (18.3 ± 4.7), as compared to the HAMA (12.0 ± 2.7 and 12.2 ± 2.8) and Untreated groups (9.8 ± 2.4 and 11.5 ± 2.1) (Fig. 7c, detailed itemized raring score in Tables 1 and 2). A similar trend was also observed for the mean intensity of collagen type II staining (Fig. 7d).

4. Discussion

Injectable adhesive hydrogel with fast, easy and efficient gelation *in situ* is required for cartilage repair surgery [22,37]. The gelation of hydrogels *in situ* enables the liquid pre-hydrogel solution to adapt to irregular cartilage defects, prior to undergoing gelation to form a hydrogel with high adhesive strength, which can preserve the maximal amount of surrounding cartilage [37]. Conventional gelation of injectable hydrogels usually involves the mixture of multiple components, which complicates the surgical operation and make the hydrogel unstable [5,22,38]. In this study, single component AHAMA hydrogel can be subjected to a one-step light-initiated gelation to fill the cartilage defect, which allows more flexibility, as well as excellent spatiotemporal control.

Seamless hydrogel-cartilage integration is critical for cartilage regeneration, as it could facilitate migration of host cells (MSCs and chondrocytes, etc.) to the defect site and promote neo-tissue formation [5,22]. However, implanted biomaterials often fail to regenerate cartilage, without good cartilage integration [4,39]. In this study, the strong adhesion of AHAMA effectively fixed the implanted scaffolds in place to maximize regeneration potential [12,40]. Through multiple adhesion sites, the implanted AHAMA hydrogel scaffold formed a seamless interface with the host tissue at the microscale level, as demonstrated by SEM (Fig. 3d and e), improving neo-tissue formation, and ultimately promoting the integration between neo-cartilage and native cartilage. More importantly, smooth transition between neo-cartilage and native cartilage was attained in the AHAMA groups, suggesting good integration between the neo-cartilage and native cartilage, which was not seen in the Untreated and HAMA groups (Figs. 6c and 7a).

There is a possibility that aldehyde groups on oxidized hyaluronic acids may compromise biocompatibility. Nevertheless, biomaterials with aldehyde groups have been widely utilized for repair surgery of cartilage and other tissues [5,18,22,41]. Not all are cytotoxic. Cytotoxicity depends on the structure and origin of the specific aldehyde group. Cytotoxicity of aldehydes are mainly attributed to α,β-unsaturated aldehydes that are endogenously produced by lipid peroxidation, such as 4-hydroxynonenal (4-HNE), acrolein, malondialdehyde (MDA) and crotonaldehyde (Cr), associated with aging [42,43], inflammation [44,45], neurological disorders [46] and cancer [43]. However, aldehydes, such as protocatechuic aldehyde [47], cinnamaldehyde [48] and

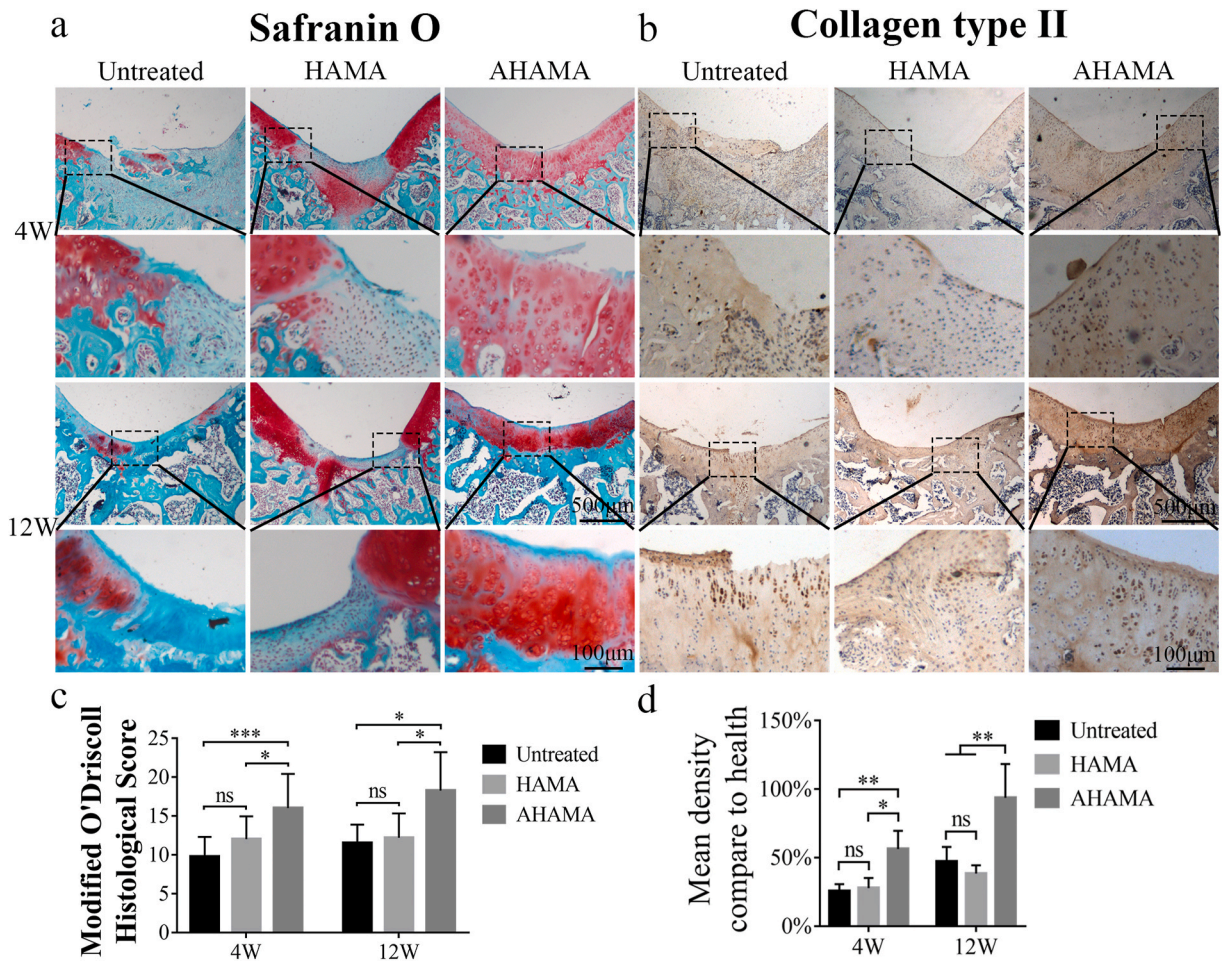

Fig. 7. Safranin O and immunohistochemistry staining of collagen type II. (a) Safranin O staining of repaired cartilage after 4- and 12-weeks post-surgery. (b) Immunohistochemistry staining of collagen type II in repaired cartilage after 4- and 12-weeks post-surgery. (c) Modified O'Driscoll histological scores (24 scores system) of Untreated, HAMA and AHAMA groups at 4- and 12-weeks post-surgery (n = 6). (d) Mean density of collagen type II staining, compared to the healthy group (n = 6, mean values ± SD, *P < 0.05, **P < 0.01, ***P < 0.001).

Table 1
Modified O'Driscoll histological evaluation of cartilage repair at 4 weeks.

Category	Untreated		HAMA		AHAMA	
	Mean	SD	Mean	SD	Mean	SD
Cellular morphology	0.25	0.66	0.57	0.90	1.43	0.90
Safranin-O staining of the matrix	0.88	0.60	1.43	0.49	2.00	0.93
Surface regularity	1.00	0.87	1.43	0.49	1.86	0.64
Structural integrity	0.50	0.50	1.00	0.00	1.71	0.45
Thickness	1.13	0.78	1.14	0.64	1.29	0.70
Bonding to the adjacent cartilage	1.25	0.66	1.14	0.83	1.71	0.45
Hypocellularity	2.88	0.33	3.00	0.00	3.00	0.00
Chondrocyte clustering	0.38	0.48	0.43	0.49	0.86	0.99
Adjacent cartilage degenerative joint disease	1.50	0.87	1.86	0.64	2.14	0.35
Total	9.75	–	12.00	–	16.00	–

Table 2
Modified O'Driscoll histological evaluation of cartilage repair at 12 weeks.

Category	Untreated		HAMA		AHAMA	
	Mean	SD	Mean	SD	Mean	SD
Cellular morphology	0.50	0.87	0.80	0.98	2.25	1.56
Safranin-O staining of the matrix	1.00	0.71	1.00	1.10	2.13	1.17
Surface regularity	1.75	0.83	1.80	0.75	2.25	1.09
Structural integrity	0.75	0.43	1.20	0.40	1.63	0.48
Thickness	1.50	0.50	1.60	0.49	1.75	0.43
Bonding to the adjacent cartilage	1.75	0.43	1.60	0.80	2.00	0.00
Hypocellularity	2.25	0.43	2.80	0.40	3.00	0.00
Chondrocyte clustering	0.00	0.00	0.20	0.40	0.88	0.78
Adjacent cartilage degenerative joint disease	2.00	0.71	1.20	0.40	2.38	0.48
Total	11.50	–	12.20	–	18.25	–

coniferyl aldehyde [49], have been shown to suppress inflammation. Oxidized hyaluronic acid with aldehyde groups have demonstrated good biocompatibility in ophthalmic applications both *in vitro* and *in vivo* [50]. In this study, aldehyde groups within repeating units of AHAMA are saturated aldehydes with negligible toxic effects. Moreover, cytotoxicity also depends on the concentration. A delicate balance exists between basal levels of aldehydes and cytotoxic threshold concentrations [51]. In this research, only 50 μL of AHAMA was injected into the cartilage defect, and the aldehyde content in the AHAMA hydrogel is quite low.

The degradation ratio of HA could be reduced through modification with some functional groups, such as methacrylate [52] or sulfate groups [53]. Moreover, there was reported to be good correlation between the degradation rate and modification degree [53,54], molecular weight of the HA [55], and cross-linking density of the hydrogel [56]. The HAMA used in this study with 24% of methacrylate modification

degree and 100 KDã200 KDa molecular weight, is supposed to have similar degradation rates reported by previous studies [52,57]. In AHAMA, the ring-opening oxidation is susceptible to hemiacetal hydrolysis and glycoside-bond cleavage in acidic medium, which slightly enhance the degradation [58]. Notably, the oxidation level of AHAMA was 36%, which means that 64% of the polymer in the AHAMA hydrogel is unoxidized HAMA. This fraction of unoxidized HAMA in the AHAMA hydrogel likely degrade at a similar rate as the HAMA, leading to similar degradation rate during the early stage [53].

5. Conclusion

In summary, we have fabricated a HA methacrylate hydrogel modified with aldehyde groups (AHAMA), which could be quickly and conveniently prepared *in situ*. This demonstrated good biocompatibility and tissue adhesion *in vitro*, and could promote integration between neocartilage and native cartilage, which significantly enhanced cartilage regeneration. Hence, AHAMA hydrogel is a promising adhesive biomaterial for clinical cartilage regeneration and other biomedical applications.

Credit Author Statement

Jiaqing Chen: conception and design, materials fabrication, collection and assembly data, data analysis and interpretation, manuscript writing, final approval of manuscript; Jiabei Yang: conception and design, manuscript writing, final approval of manuscript; Li Wang: data interpretation, manuscript writing and final approval of manuscript; Xuewei Zhang: data interpretation, manuscript writing and final approval of manuscript; Boon Chin Heng: manuscript writing; Dong-An Wang: manuscript writing; Zigang Ge: conception and design, manuscript writing, final approval of manuscript.

Declaration of competing interest

The authors hereby declare that they have no competing interests.

Acknowledgements

This work was supported by the National Natural Science Foundation of China grant (81772334) and Peking University Medicine Seed Fund for Interdisciplinary Research (BMU2018ME001).

Appendix A. Supplementary data

Supplementary data to this article can be found online at https://doi.org/10.1016/j.bioactmat.2020.11.020.

References

[1] J. Li, A.D. Celiz, J. Yang, Q. Yang, I. Wamala, W. Whyte, B.R. Seo, N.V. Vasilyev, J. J. Vlassak, Z. Suo, D.J. Mooney, Tough adhesives for diverse wet surfaces, Science 357 (6349) (2017) 378–381, https://doi.org/10.1126/science.aah6362.

[2] Y.L. Yang, J.Y. Zhang, Z.Z. Liu, Q.N. Lin, X.L. Liu, C.Y. Bao, Y. Wang, L.Y. Zhu, Tissue-integratable and biocompatible photogelation by the imine crosslinking reaction, Adv. Mater. 28 (14) (2016) 2724–2730, https://doi.org/10.1002/adma.201505336.

[3] W. Wei, Y. Ma, X. Yao, W. Zhou, X. Wang, C. Li, J. Lin, Q. He, S. Leptihn, H. Ouyang, Advanced hydrogels for the repair of cartilage defects and regeneration, Bioact Mater 6 (4) (2021) 998–1011, https://doi.org/10.1016/j.bioactmat.2020.09.030.

[4] D.A. Wang, S. Varghese, B. Sharma, I. Strehin, S. Fermanian, J. Gorham, D. H. Fairbrother, B. Cascio, J.H. Elisseeff, Multifunctional chondroitin sulphate for cartilage tissue-biomaterial integration, Nat. Mater. 6 (5) (2007) 385–392, https://doi.org/10.1038/nmat1890.

[5] X.L. Liu, Y.L. Yang, X. Niu, Q.N. Lin, B.Z. Zhao, Y. Wang, L.Y. Zhu, An in situ photocrosslinkable platelet rich plasma - complexed hydrogel glue with growth factor controlled release ability to promote cartilage defect repair, Acta Biomater. 62 (2017) 179–187, https://doi.org/10.1016/j.actbio.2017.05.023.

[6] W.D. Spotnitz, S. Burks, Hemostats, sealants, and adhesives: components of the surgical toolbox, Transfusion 48 (7) (2008) 1502–1516, https://doi.org/10.1111/j.1537-2995.2008.01703.x.

[7] D.H. Sierra, Fibrin sealant adhesive systems: a review of their chemistry, material properties and clinical applications, J. Biomater. Appl. 7 (4) (1993) 309–352, https://doi.org/10.1177/088532829300700402.

[8] D.G. Wallace, G.M. Cruise, W.M. Rhee, J.A. Schroeder, J.J. Prior, J. Ju, M. Maroney, J. Duronio, M.H. Ngo, T. Estridge, G.C. Coker, A tissue sealant based on reactive multifunctional polyethylene glycol, J. Biomed. Mater. Res. 58 (5) (2001) 545–555.

[9] A.K. Dastjerdi, M. Pagano, M.T. Kaartinen, M.D. McKee, F. Barthelat, Cohesive behavior of soft biological adhesives: experiments and modeling, Acta Biomater. 8 (9) (2012) 3349–3359, https://doi.org/10.1016/j.actbio.2012.05.005.

[10] H. Vinters, K. Galil, M. Lundie, J. Kaufmann, The histotoxicity of cyanoacrylates, Neuroradiology 27 (4) (1985) 279–291.

[11] C. Ghobril, M.W. Grinstaff, The chemistry and engineering of polymeric hydrogel adhesives for wound closure: a tutorial, Chem. Soc. Rev. 44 (7) (2015) 1820–1835, https://doi.org/10.1039/c4cs00332b.

[12] H.J. Faust, S.D. Sommerfeld, S. Rathod, A. Rittenbach, S.R. Banerjee, B.M.W. Tsui, M. Pomper, M.L. Amzel, A. Singh, J.H. Elisseeff, A hyaluronic acid binding peptide-polymer system for treating osteoarthritis, Biomaterials 183 (2018) 93–101, https://doi.org/10.1016/j.biomaterials.2018.08.045.

[13] C. Qi, J. Liu, Y. Jin, L.M. Xu, G.B. Wang, Z. Wang, L. Wang, Photo-crosslinkable, injectable sericin hydrogel as 3D biomimetic extracellular matrix for minimally invasive repairing cartilage, Biomaterials 163 (2018) 89–104, https://doi.org/10.1016/j.biomaterials.2018.02.016.

[14] P. Karami, C.S. Wyss, A. Khoushabi, A. Schmocker, M. Broome, C. Moser, P. E. Bourban, D.P. Pioletti, Composite double-network hydrogels to improve adhesion on biological surfaces, Acs Appl Mater Inter 10 (45) (2018) 38692–38699, https://doi.org/10.1021/acsami.8b10735.

[15] G.C. Ingavle, S.H. Gehrke, M.S. Detamore, The bioactivity of agarose-PEGDA interpenetrating network hydrogels with covalently immobilized RGD peptides and physically entrapped aggrecan, Biomaterials 35 (11) (2014) 3558–3570, https://doi.org/10.1016/j.biomaterials.2014.01.002.

[16] C.S.D. Lee, J.P. Gleghorn, N.W. Choi, M. Cabodi, A.D. Stroock, L.J. Bonassar, Integration of layered chondrocyte-seeded alginate hydrogel scaffolds, Biomaterials 28 (19) (2007) 2987–2993, https://doi.org/10.1016/j.biomaterials.2007.02.035.

[17] R.C. Pereira, M. Scaranari, P. Castagnola, M. Grandizio, H.S. Azevedo, R.L. Reis, R. Cancedda, C. Gentili, Novel injectable gel (system) as a vehicle for human articular chondrocytes in cartilage tissue regeneration, J Tissue Eng Regen M 3 (2) (2009) 97–106, https://doi.org/10.1002/term.145.

[18] F. Yu, X. Cao, J. Du, G. Wang, X. Chen, Multifunctional hydrogel with good structure integrity, self-healing, and tissue-adhesive property formed by combining diels-alder click reaction and acylhydrazone bond, ACS Appl. Mater. Interfaces 7 (43) (2015) 24023–24031, https://doi.org/10.1021/acsami.5b06896.

[19] F. Chen, Y.Z. Ni, B. Liu, T.T. Zhou, C.Y. Yu, Y. Su, X.Y. Zhu, X.W. Yu, Y.F. Zhou, Self-crosslinking and injectable hyaluronic acid/RGD-functionalized pectin hydrogel for cartilage tissue engineering, Carbohydr. Polym. 166 (2017) 31–44, https://doi.org/10.1016/j.carbpol.2017.02.059.

[20] J.K. Xu, G.M. Soliman, J. Barralet, M. Cerruti, Mollusk glue inspired mucoadhesives for biomedical applications, Langmuir 28 (39) (2012) 14010–14017, https://doi.org/10.1021/la3025414.

[21] H. Meng, Y.T. Li, M. Faust, S. Konst, B.P. Lee, Hydrogen peroxide generation and biocompatibility of hydrogel-bound mussel adhesive moiety, Acta Biomater. 17 (2015) 160–169, https://doi.org/10.1016/j.actbio.2015.02.002.

[22] F.F. Zhou, Y. Hong, X.Z. Zhang, L. Yang, J. Li, D.M. Jiang, V. Bunpetch, Y.J. Hu, H. W. Ouyang, S.F. Zhang, Tough hydrogel with enhanced tissue integration and in situ forming capability for osteochondral defect repair, Appl Mater Today 13 (2018) 32–44, https://doi.org/10.1016/j.apmt.2018.08.005.

[23] Y.Y. Duan, X.G. Li, X.G. Zuo, T. Shen, S. Yu, L.H. Deng, C.Y. Gao, Migration of endothelial cells and mesenchymal stem cells into hyaluronic acid hydrogels with different moduli under induction of pro-inflammatory macrophages, J. Mater. Chem. B 7 (36) (2019) 5478–5489, https://doi.org/10.1039/c9tb01126a.

[24] P. Bulpitt, D. Aeschlimann, New strategy for chemical modification of hyaluronic acid: preparation of functionalized derivatives and their use in the formation of novel biocompatible hydrogels, J. Biomed. Mater. Res. 47 (2) (1999) 152–169.

[25] H.P. Tan, C.R. Chu, K.A. Payne, K.G. Marra, Injectable in situ forming biodegradable chitosan-hyaluronic acid based hydrogels for cartilage tissue engineering, Biomaterials 30 (13) (2009) 2499–2506, https://doi.org/10.1016/j.biomaterials.2008.12.080.

[26] T. Ito, Y. Yeo, C.B. Highley, E. Bellas, C.A. Benitez, D.S. Kohane, The prevention of peritoneal adhesions by in situ cross-linking hydrogels of hyaluronic acid and cellulose derivatives, Biomaterials 28 (6) (2007) 975–983, https://doi.org/10.1016/j.biomaterials.2006.10.021.

[27] K. Kawasaki, M. Ochi, Y. Uchio, N. Adachi, M. Matsusaki, Hyaluronic acid enhances proliferation and chondroitin sulfate synthesis in cultured chondrocytes embedded in collagen gels, J. Cell. Physiol. 179 (2) (1999) 142–148, https://doi.org/10.1002/(SICI)1097-4652(199905)179:2<142:AID-JCP4>3.0.CO;2-Q.

[28] A.A. Hegewald, J. Ringe, J. Bartel, I. Kruger, M. Notter, D. Barnewitz, C. Kaps, M. Sittinger, Hyaluronic acid and autologous synovial fluid induce chondrogenic differentiation of equine mesenchymal stem cells: a preliminary study, Tissue Cell 36 (6) (2004) 431–438, https://doi.org/10.1016/j.tice.2004.07.003.

[29] B. Gerdin, R. Hallgren, Dynamic role of hyaluronan (HYA) in connective tissue activation and inflammation, J. Intern. Med. 242 (1) (1997) 49–55, https://doi.org/10.1046/j.1365-2796.1997.00173.x.

[30] Y. Kusayama, Y. Akamatsu, K. Kumagai, H. Kobayashi, A. Nakazawa, T. Saito, Changes of the biomarkers in synovial fluid and clinical efficacy of intra-articular injection hyaluronic acid for patients with knee osteoarthritis, Osteoarthritis Cartilage 22 (2014) S478–S479, https://doi.org/10.1016/j.joca.2014.02.909.
[31] A. Singh, M. Corvelli, S.A. Unterman, K.A. Wepasnick, P. McDonnell, J.H. Elisseeff, Enhanced lubrication on tissue and biomaterial surfaces through peptide-mediated binding of hyaluronic acid, Nat. Mater. 13 (10) (2014) 988–995, https://doi.org/10.1038/Nmat4048.
[32] H.P. Tan, H. Li, J.P. Rubin, K.G. Marra, Controlled gelation and degradation rates of injectable hyaluronic acid-based hydrogels through a double crosslinking strategy, J Tissue Eng Regen M 5 (10) (2011) 790–797, https://doi.org/10.1002/term.378.
[33] H.P. Tan, J.P. Rubin, K.G. Marra, Injectable in situ forming biodegradable chitosan-hyaluronic acid based hydrogels for adipose tissue regeneration, Organogenesis 6 (3) (2010) 173–180, https://doi.org/10.4161/org.6.3.12037.
[34] K.A. Smeds, A. Pfister-Serres, D. Miki, K. Dastgheib, M. Inoue, D.L. Hatchell, M. W. Grinstaff, Photocrosslinkable polysaccharides for in situ hydrogel formation, J. Biomed. Mater. Res. B Appl. Biomater. 54 (1) (2001) 115–121.
[35] A.R. Narkar, B. Barker, M. Clisch, J.F. Jiang, B.P. Lee, pH responsive and oxidation resistant wet adhesive based on reversible catechol-boronate complexation, Chem. Mater. 28 (15) (2016) 5432–5439, https://doi.org/10.1021/acs.chemmater.6b01851.
[36] L. Li, N. Wang, X. Jin, R. Deng, S.H. Nie, L. Sun, Q.J. Wu, Y.Q. Wei, C.Y. Gong, Biodegradable and injectable in situ cross-linking chitosan-hyaluronic acid based hydrogels for postoperative adhesion prevention, Biomaterials 35 (12) (2014) 3903–3917, https://doi.org/10.1016/j.biomaterials.2014.01.050.
[37] B. Sharma, S. Fermanian, M. Gibson, S. Unterman, D.A. Herzka, B. Cascio, J. Coburn, A.Y. Hui, N. Marcus, G.E. Gold, J.H. Elisseeff, Human cartilage repair with a photoreactive adhesive-hydrogel composite, Sci. Transl. Med. 5 (167) (2013). ARTN.167ra6.10.1126/scitranslmed.3004838.
[38] M.C. Giano, Z. Ibrahim, S.H. Medina, K.A. Sarhane, J.M. Christensen, Y. Yamada, G. Brandacher, J.P. Schneider, Injectable bioadhesive hydrogels with innate antibacterial properties, Nat. Commun. 5 (2014) 4095, https://doi.org/10.1038/ncomms5095.
[39] K.L. Spiller, S.A. Maher, A.M. Lowman, Hydrogels for the repair of articular cartilage defects, Tissue Eng. B Rev. 17 (4) (2011) 281–299, https://doi.org/10.1089/ten.teb.2011.0077.
[40] T.A. Schmidt, N.S. Gastelum, Q.T. Nguyen, B.L. Schumacher, R.L. Sah, Boundary lubrication of articular cartilage - role of synovial fluid constituents, Arthritis Rheum-Us 56 (3) (2007) 882–891, https://doi.org/10.1002/art.22446.
[41] Y. Hong, F.F. Zhou, Y.J. Hua, X.Z. Zhang, C.Y. Ni, D.H. Pan, Y.Q. Zhang, D. M. Jiang, L. Yang, Q.N. Lin, Y.W. Zou, D.S. Yu, D.E. Arnot, X.H. Zou, L.Y. Zhu, S. F. Zhang, H.W. Ouyang, A strongly adhesive hemostatic hydrogel for the repair of arterial and heart bleeds, Nat. Commun. 10 (2019). ARTN206010.1038/s41467-019-10004-7.
[42] L.F. Dmitriev, V.N. Titov, Lipid peroxidation in relation to ageing and the role of endogenous aldehydes in diabetes and other age-related diseases, Ageing Res. Rev. 9 (2) (2010) 200–210, https://doi.org/10.1016/j.arr.2009.09.004.
[43] G.P. Voulgaridou, I. Anestopoulos, R. Franco, M.I. Panayiotidis, A. Pappa, DNA damage induced by endogenous aldehydes: current state of knowledge, Mutat Res-Fund Mol M 711 (1–2) (2011) 13–27, https://doi.org/10.1016/j.mrfmmm.2011.03.006.
[44] Y.M. Go, P.J. Halvey, J.M. Hansen, M. Reed, J. Pohl, D.P. Jones, Reactive aldehyde modification of thioredoxin-1 activates early steps of inflammation and cell adhesion, Am. J. Pathol. 171 (5) (2007) 1670–1681, https://doi.org/10.2353/ajpath.2007.070218.
[45] D.T. Antoniak, M.J. Duryee, T.R. Mikuls, G.M. Thiele, D.R. Anderson, Aldehyde-modified proteins as mediators of early inflammation in atherosclerotic disease, Free Radical Biol. Med. 89 (2015) 409–418, https://doi.org/10.1016/j.freeradbiomed.2015.09.003.
[46] M. Trevisani, J. Siemens, S. Materazzi, D.M. Bautista, R. Nassini, B. Campi, N. Imamachi, E. Andre, R. Patacchini, G.S. Cottrell, R. Gatti, A.I. Basbaum, N. W. Bunnett, D. Julius, P. Geppetti, 4-Hydroxynonenal, an endogenous aldehyde, causes pain and neurogenic inflammation through activation of the irritant receptor TRPA1, P Natl Acad Sci USA 104 (33) (2007) 13519–13524, https://doi.org/10.1073/pnas.0705923104.
[47] L. Gao, W.F. Wu, L. Dong, G.L. Ren, H.D. Li, Q. Yang, X.F. Li, T. Xu, Z. Li, B.M. Wu, T.T. Ma, C. Huang, Y. Huang, L. Zhang, X.W. Lv, J. Li, X.M. Meng, Protocatechuic aldehyde attenuates cisplatin-induced acute kidney injury by suppressing nox-mediated oxidative stress and renal inflammation, Front. Pharmacol. 7 (2016). ARTN.479.10.3389/fphar.2016.00479.
[48] P. Khare, S. Jagtap, Y. Jain, R.K. Baboota, P. Mangal, R.K. Boparai, K.K. Bhutani, S. S. Sharma, L.S. Premkumar, K.K. Kondepudi, K. Chopra, M. Bishnoi, Cinnamaldehyde supplementation prevents fasting-induced hyperphagia, lipid accumulation, and inflammation in high-fat diet-fed mice, Biofactors 42 (2) (2016) 201–211, https://doi.org/10.1002/biof.1265.
[49] M. Akram, K.A. Kim, E.S. Kim, Y.J. Shin, D. Noh, E. Kim, J.H. Kim, A. Majid, S. Y. Chang, J.K. Kim, O.N. Bae, Selective inhibition of JAK2/STAT1 signaling and iNOS expression mediates the anti-inflammatory effects of coniferyl aldehyde, Chem. Biol. Interact. 256 (2016) 102–110, https://doi.org/10.1016/j.cbi.2016.06.029.
[50] J.Y. Lai, D.H.K. Ma, Ocular biocompatibility of gelatin microcarriers functionalized with oxidized hyaluronic acid, Mat Sci Eng C-Mater 72 (2017) 150–159, https://doi.org/10.1016/j.msec.2016.11.067.
[51] K.S. Fritz, D.R. Petersen, An overview of the chemistry and biology of reactive aldehydes, Free Radical Biol. Med. 59 (2013) 85–91, https://doi.org/10.1016/j.freeradbiomed.2012.06.025.
[52] C. Chung, M. Beecham, R.L. Mauck, J.A. Burdick, The influence of degradation characteristics of hyaluronic acid hydrogels on in vitro neocartilage formation by mesenchymal stem cells, Biomaterials 30 (26) (2009) 4287–4296, https://doi.org/10.1016/j.biomaterials.2009.04.040.
[53] Q. Feng, S. Lin, K.Y. Zhang, C.Q. Dong, T.Y. Wu, H.Q. Huang, X.H. Yan, L. Zhang, G. Li, L.M. Bian, Sulfated hyaluronic acid hydrogels with retarded degradation and enhanced growth factor retention promote hMSC chondrogenesis and articular cartilage integrity with reduced hypertrophy, Acta Biomater. 53 (2017) 329–342, https://doi.org/10.1016/j.actbio.2017.02.015.
[54] J.B. Leach, K.A. Bivens, C.W. Patrick, C.E. Schmidt, Photocrosslinked hyaluronic acid hydrogels: natural, biodegradable tissue engineering scaffolds, Biotechnol. Bioeng. 82 (5) (2003) 578–589, https://doi.org/10.1002/bit.10605.
[55] R. Jin, L.S.M. Teixeira, A. Krouwels, P.J. Dijkstra, C.A. van Blitterswijk, M. Karperien, J. Feijen, Synthesis and characterization of hyaluronic acid-poly (ethylene glycol) hydrogels via Michael addition: an injectable biomaterial for cartilage repair, Acta Biomater. 6 (6) (2010) 1968–1977, https://doi.org/10.1016/j.actbio.2009.12.024.
[56] J.A. Burdick, C. Chung, X.Q. Jia, M.A. Randolph, R. Langer, Controlled degradation and mechanical behavior of photopolymerized hyaluronic acid networks, Biomacromolecules 6 (1) (2005) 386–391, https://doi.org/10.1021/bm049508a.
[57] C. Schramm, M.S. Spitzer, S. Henke-Fahle, G. Steinmetz, K. Januschowski, P. Heiduschka, J. Geis-Gerstorfer, T. Biedermann, K.U. Bartz-Schmidt, P. Szurman, The cross-linked biopolymer hyaluronic acid as an artificial vitreous substitute, Invest. Ophthalmol. Vis. Sci. 53 (2) (2012) 613–621, https://doi.org/10.1167/iovs.11-7322.
[58] T. Hozumi, T. Kageyama, S. Ohta, J. Fukuda, T. Ito, Injectable hydrogel with slow degradability composed of gelatin and hyaluronic acid cross-linked by schiff's base formation, Biomacromolecules 19 (2) (2018) 288–297, https://doi.org/10.1021/acs.biomac.7b01133.